MINNESOTA GEOLOGICAL SURVEY

PRISCILLA C. GREW, *Director*

TOURMALINE IN EARLY PROTEROZOIC METASEDIMENTARY ROCKS NEAR PHILBROOK, NORTHEASTERN TODD COUNTY, CENTRAL MINNESOTA

Terrence J. Boerboom

Report of Investigations 38
ISSN 0076-9177

UNIVERSITY OF MINNESOTA

Saint Paul — 1989

CONTENTS

ILLUSTRATIONS

TABLES

TOURMALINE IN EARLY PROTEROZOIC METASEDIMENTARY ROCKS NEAR PHILBROOK, NORTHEASTERN TODD COUNTY, CENTRAL MINNESOTA

By

Terrence J. Boerboom

ABSTRACT

A sequence of Early Proterozoic metasedimentary rocks near the town of Philbrook, at the northwestern edge of the Animikie basin, has been correlated with the lower part of the Mille Lacs Group. These rocks, which were deformed during the Penokean orogeny, contain elevated amounts of tourmaline and thin beds of tourmalinite, which have been recognized elsewhere to be associated with stratabound, sediment-hosted massive sulfide deposits.

The Philbrook sequence is confined entirely to the subsurface. It consists of arkose, chlorite–muscovite schist, iron-formation, and minor volumes of other mafic schist types. Small nearby outcrops consist of tonalitic basement rock (Archean) unconformably overlain by conglomerate (Early Proterozoic). The iron-formation produces a strong positive magnetic anomaly that was first recognized by dip-needle surveys, and was drilled in the early 1900s for iron ore. The sequence strikes north-northwest and dips steeply to the east. Tourmaline is most abundant in the arkosic rocks and in the chlorite–muscovite schist.

The iron-formation is thinly laminated, and individual laminae range from less than 1 mm to 7 mm in thickness. Bedding is defined by clastic-dominated and chert-dominated laminae, which contain internal laminae of varying ratios of quartz to Fe-oxide minerals. The arkosic rocks do not contain recognizable bedding features, but primary sedimentary grain shapes are visible in thin section. The arkose contains albite (An_{05}) that is weakly to heavily sericitized, and feldspar-quartz ratios range from 1.5:1 to 9:1 and average 3:1. The chlorite–muscovite schist contains iron-formation laminae as thick as 1 cm and locally grades into iron-formation. Other varieties of schist contain abundant carbonate and variable amounts of epidote, chlorite, and actinolite; these are derived partially or wholly from mafic volcanic rocks or thin hypabyssal mafic sills.

Bluish-green tourmaline with thin overgrowth rims and magnetite and quartz inclusions makes up as much as 2% of the chlorite–muscovite schist. It occurs as disseminated crystals, and also in weakly defined beds with magnetite. Brown tourmaline occurs in the arkosic rocks; it has thin overgrowth rims, but generally is inclusion-free. It occurs as disseminated grains and as thin tourmalinite laminae ranging from 0.5 mm to 1.5 mm in thickness that contain as much as 50% tourmaline. Chemical analyses of both tourmaline color types show they have compositions between schorl (Fe end-member) and dravite (Mg end-member), with an additional uvite (Ca end-member) component in the brown tourmaline.

Tourmaline associated with stratiform settings at other localities shows a distinctly more magnesian composition than tourmaline from igneous settings. Detailed studies of tourmaline from the host rocks of massive sulfide orebodies and from barren stratiform tourmalinites show the tourmaline to have a slightly higher Fe/(Fe+Mg) ratio than tourmaline from ore zones. The composition of Philbrook tourmaline is similar to both of the former, and suggests that the Philbrook sequence either is barren, or possibly is the host rock for a nearby sulfide occurrence.

Tourmalinites and associated massive sulfide deposits typically occur in argillaceous or arenaceous sediments in Proterozoic or Early Paleozoic rift basins. The boron (and metals) are thought to have been concentrated in a fault-controlled, hydrothermal vent system by leaching from the sedimentary pile and redeposition at submarine vents. These processes are compatible with the probable tectonosedimentary processes at Philbrook.

INTRODUCTION

Early Proterozoic metasedimentary rocks near Philbrook in Todd County of east-central Minnesota were first recognized in the general literature by Morey (1978), who mapped them as an outlier located some 15 km west of the Animikie basin. Except for a few scattered small outcrops of conglomerate, the metasedimentary rocks are buried by as much as 50 m of Pleistocene glacial materials.

Recent geologic mapping by Southwick and others (1988) has greatly clarified the structural position of the Philbrook sequence. They have shown that the metasedimentary rocks near Philbrook were deposited along the northwestern edge of what became an extension of the Animikie basin (Figs. 1 and 2), and subsequently isoclinally folded and faulted during the Penokean orogeny, a major deformational event at about 1850 Ma. Because of extensive folding and faulting, the stratigraphic position of the Philbrook sequence relative to other rocks in the Animikie basin is uncertain. However, Morey (1978) and Southwick and others (1988) tentatively correlate the Philbrook sequence with the lower part of the Mille Lacs Group, a sequence of dominantly quartz-rich arenite and siltstone exposed in the vicinity of Mille Lacs Lake, approximately 100 km east of Philbrook.

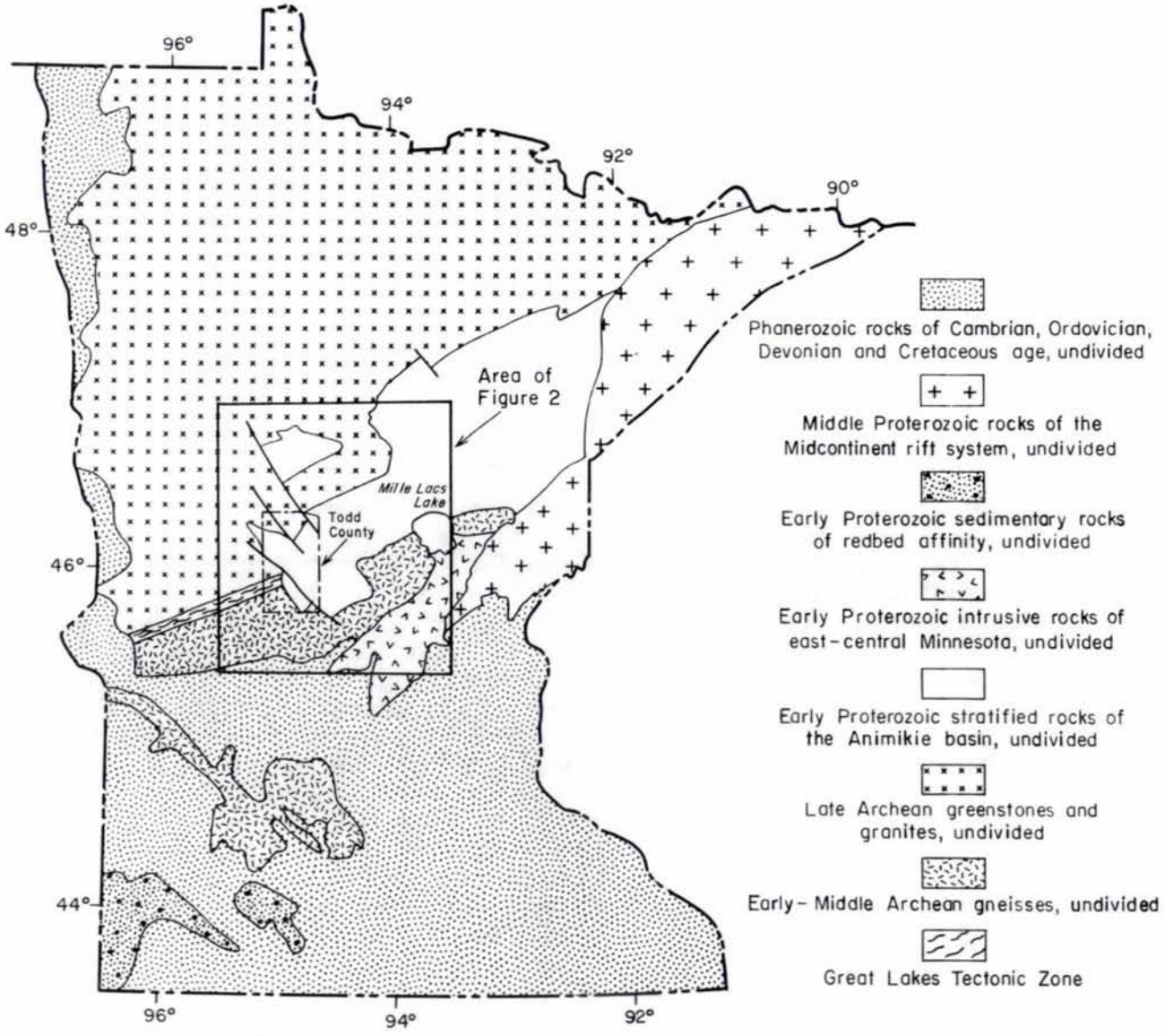

Figure 1. Generalized bedrock geologic map of Minnesota showing major Precambrian rock units (modified from Dacre and others, 1984; Southwick and others, 1988). Box shows area of Figure 2.

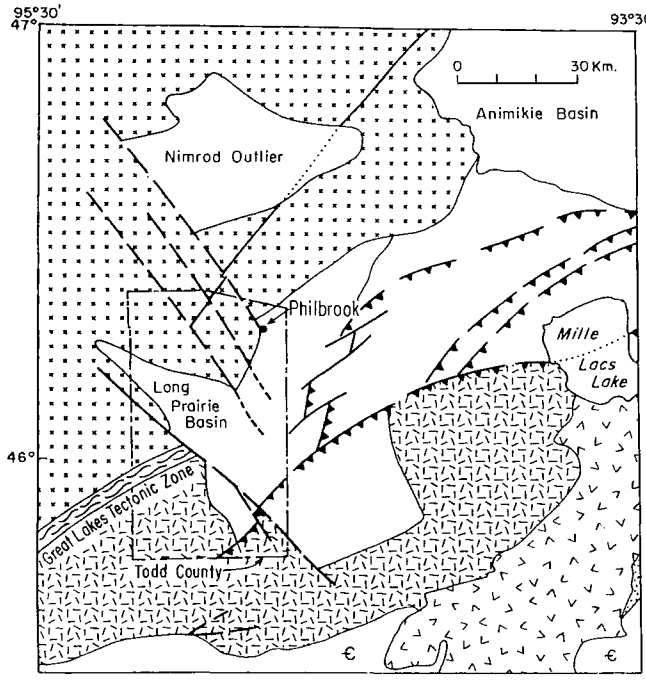

Figure 2. Geologic map of a part of central Minnesota (modified from Dacre and others, 1984; Southwick and others, 1988). See Figure 1 for key to rock symbols.

The Philbrook sequence has many attributes similar to those in other Early Proterozoic sequences in east-central Minnesota. However, it is unique in that it contains beds of tourmalinite, a name coined by Slack and others (1984) for "stratabound lithological units concordant with their enclosing host rocks and containing 15% to 20% or more tourmaline by volume."

Tourmalinites have not been described previously from Minnesota, but Schmidt (1963) did recognize argillaceous beds in the Early Proterozoic Trommald Formation of the Cuyuna North range which contain as much as 10% tourmaline and as much as 0.6% boron. In the early 1960s, when Schmidt completed his study of the North range, tourmaline-bearing beds in sedimentary sequences were more or less a curiosity, vaguely ascribed to "hydrothermal" processes. However in the last few years it has been recognized that tourmalinites are typically associated with stratabound massive sulfide deposits (Ethier and Campbell, 1977) and also with stratiform scheelite deposits (Plimer, 1987). The tourmaline in these deposits is relatively Mg-rich and different from the iron-rich varieties typically associated with igneous rocks. Consequently it is possible that the Philbrook sequence may be the site of stratabound sulfide mineralization. The possibility is supported by the similarity of the Philbrook tourmalines to the tourmalines associated with known sulfide deposits at the Sullivan mine in British Columbia (Nesbitt and others, 1984), the Golden Dyke Dome in Australia (Plimer, 1986), and other localities. Moreover, associated rock types, the probable tectonic setting and depositional environment, and the age of the Philbrook sequence are analogous to those associated with stratabound sulfide deposits elsewhere. Consequently we suggest that the Philbrook area in particular, and the northwestern side of the Animikie basin in general, be evaluated for sulfide mineralization. Toward that end, we summarize in this report what is currently known about the stratigraphy, petrography, and petrology of the Philbrook sequence with particular emphasis on the tourmaline-bearing beds.

GEOLOGIC SETTING

Outcrops in the Philbrook area are relatively rare. Consequently the nature of the basement upon which the Early Proterozoic rocks were deposited is conjectural. However, several small outcrops of inferred basement and conglomerate occur east of Philbrook in sec. 34, T. 133 N., R. 32 W., along the Long Prairie River (Fig. 3).

Basement in the Philbrook area appears to be chiefly tonalite, which crops out near a tonalite-bearing conglomerate. The tonalite has not been dated radiometrically, but is assigned an Archean age on the basis of regional geologic relationships, composition, and metamorphic grade. It is typically porphyritic, and is characterized by tabular phenocrysts as long as 1 cm of oligoclase to andesine, or perthite. These well-twinned and normally zoned crystals collectively compose about 10% of the rock. The oligoclase and andesine grains are variably altered to epidote and actinolite, whereas the perthite grains are ubiquitously but weakly altered to a fine reddish product, presumably hematite-stained sericite. The groundmass is fine grained and is composed mostly of perthite, albite-twinned plagioclase, recrystallized granoblastic quartz, and red-brown biotite. Minor phases include rims of granular sphene on opaque oxides, and concentrations along fractures of chlorite, epidote, and biotite. The texture and mineralogy are indicative of an intrusive rock, as is the presence of a small inclusion that probably is a piece of wall rock incorporated into the magma. Lath-shaped plagioclase phenocrysts as long 1 cm compose 20% to 30% of this inclusion in a fine-grained, biotite-rich, relatively quartz-poor matrix.

Other outcrops in the Philbrook area include a unit of clast-supported tonalitic conglomerate, as well as a considerably different unit of quartz-rich conglomerate.

Tonalite-bearing conglomerate crops out a short distance from the tonalite outcrops proper. The exposed conglomerate is characterized by clasts which range in size from 1 to 15 cm. A few of the clasts are identical in texture and mineralogy to the tonalite proper, but most of them contain graphically intergrown quartz and perthite. Approximately

10% of the clasts are fine-grained, mafic metavolcanic rock fragments that characteristically are composed of decussate epidote, sphene, actinolite, and opaque oxides. Groundmass material consists of semi-granoblastic aggregates of quartz and feldspar of various types, plus biotite, chlorite, epidote, sphene, and some green hornblende. The biotite is the dominant mafic mineral and is concentrated into planes that anastomose between clasts.

The quartz-rich conglomerate material crops out some 300 m west of the tonalitic conglomerate. Approximately 5 m of strata are exposed in several low knobs in the Long Prairie River and in a 1-m cliff along the north bank. All of the outcrops are siliceous in appearance and hardness and have a north-northwest-trending hackly fracture cleavage. The conglomerate is characterized by angular to rounded clasts from 0.5 to 15 cm in diameter. A variety of clast lithologies includes quartzite, trachytic metavolcanic rock, Al-rich metapelite, and metasiltstone. The trachytic rock has relict amygdules and flow bands, and is composed almost entirely of fine-grained K-feldspar and decussate actinolite, along with minor quartz, sphene, epidote, and opaque oxides. Chloritoid is present in the metapelite with chlorite and epidote, in a very fine grained matrix of quartz and feldspar. A minor clast component includes a coarse-grained perthitic granite which is distinctly different from the tonalitic material. The clasts are set in a light-green, vitreous groundmass, which appears to be a fine-grained, metamorphosed siltstone. The light-green color is imparted by abundant fine needles of actinolite (Fig. 4).

The Philbrook sequence proper is confined entirely to the subsurface. It consists dominantly of arkose, iron-formation, magnetite- and tourmaline-bearing chlorite-muscovite schist, and several varieties of mafic schist. The units of iron-formation are strongly magnetic and are the cause of a pronounced linear, north-trending positive magnetic anomaly that was first recognized by dip-needle surveys in the early 1900s. Consequently the anomaly, which is located in sec. 5, T. 132 N., R. 32 W. and sec. 32, T. 133 N., R. 32 W. (Figs. 3 and 5), was extensively drilled by the Adams Mining Company in the search for iron ore. Some 33 holes were drilled between December 18, 1909 and April 15, 1910. Selected samples ranging in length from 8 cm to 30 cm were retained from each 5 feet (152 cm) of core drilled. The Adams estate has given the preserved material to the Minnesota Geological Survey.

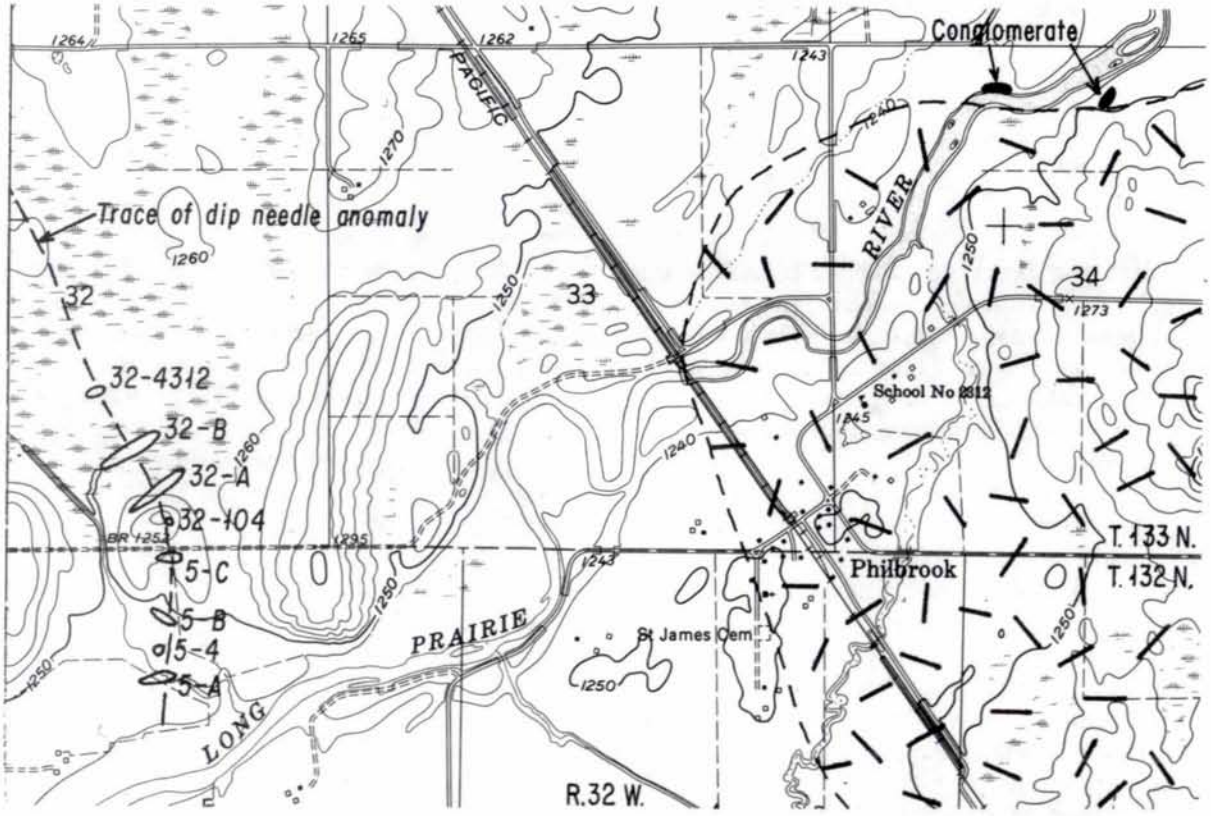

Figure 3. Drill hole and outcrop location map. Patterned area is a small mafic intrusion which is exposed in several places near Philbrook (Boerboom, 1987). Base from U.S. Geological Survey, Motley 7.5-minute quadrangle.

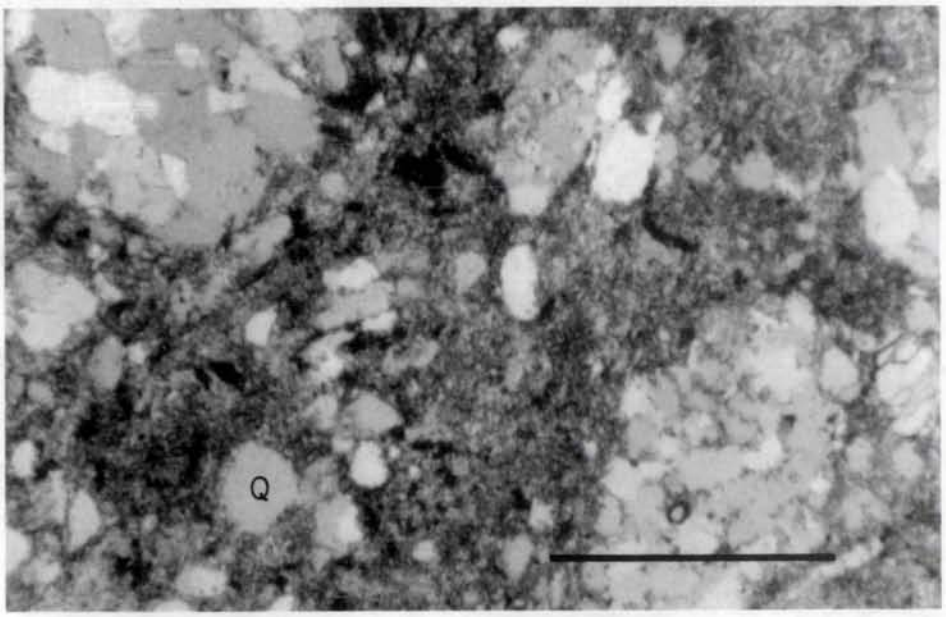

Figure 4. Quartz-rich conglomerate containing quartzite clasts (Q) in a fine-grained pelitic matrix. Bar scale 1 mm, partially crossed nicols. From outcrop on north side of Long Prairie River, NE1/4NW1/4 sec. 34, T. 133 N., R. 32 W.

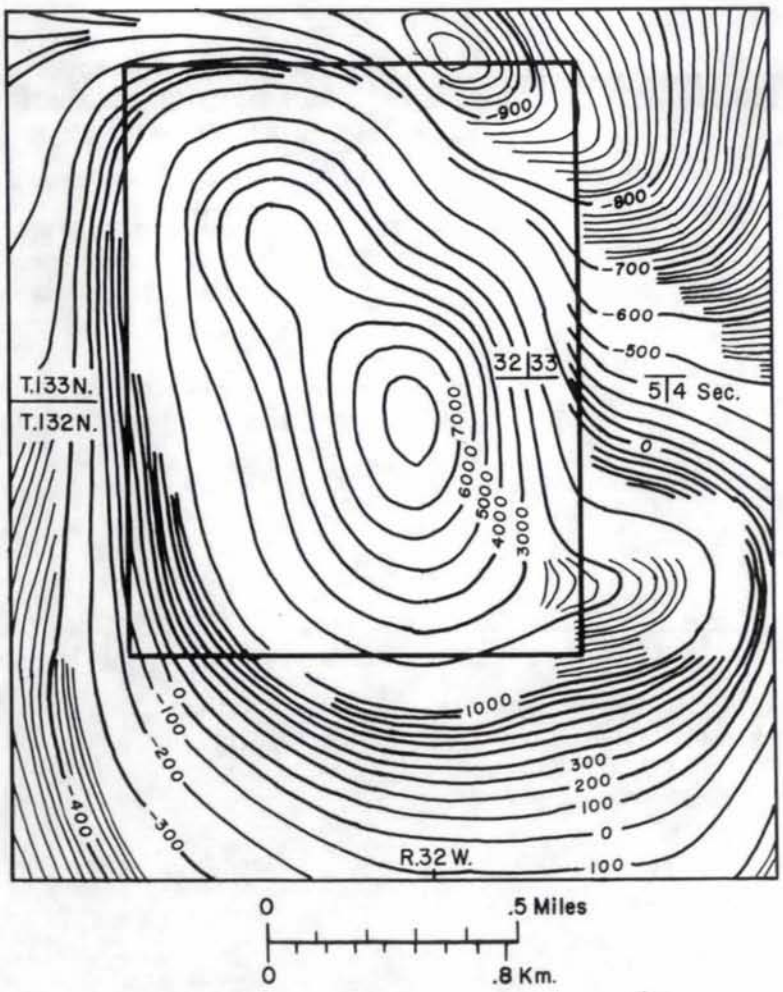

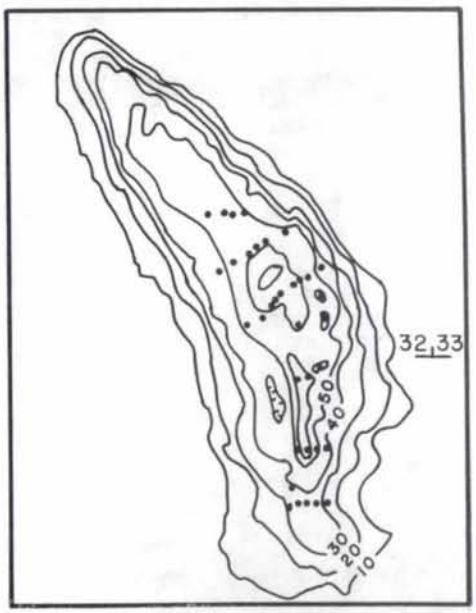

Figure 5. Aeromagnetic map (left) and ground magnetic contour map over Philbrook sequence. Dots show locations of drill holes (see Fig. 6). Aeromagnetic map from Chandler, 1984; ground map contoured from dip needle survey by Adams Mining Company in the early 1900s, originals on file at Minnesota Geological Survey.

Geologic interpretation by the Adams Mining Company inferred that the Philbrook sequence strikes to the north and northwest and dips steeply to the east, and that it consists of "quartzite" and iron-formation. Although the lack of continuous core hampers any stratigraphic interpretation, we infer that the sequence consists predominantly of arkose (Figs. 6 and 7). Approximately 30% consists of iron-formation, and about 15% is magnetite-rich chlorite–muscovite schist. Calcite-rich mafic schists, in part metamorphosed mafic volcanic rocks, make up the remainder of the sequence.

Arkose forms both the footwall and hanging wall to the main iron-bearing unit (Fig. 7). Individual sedimentation

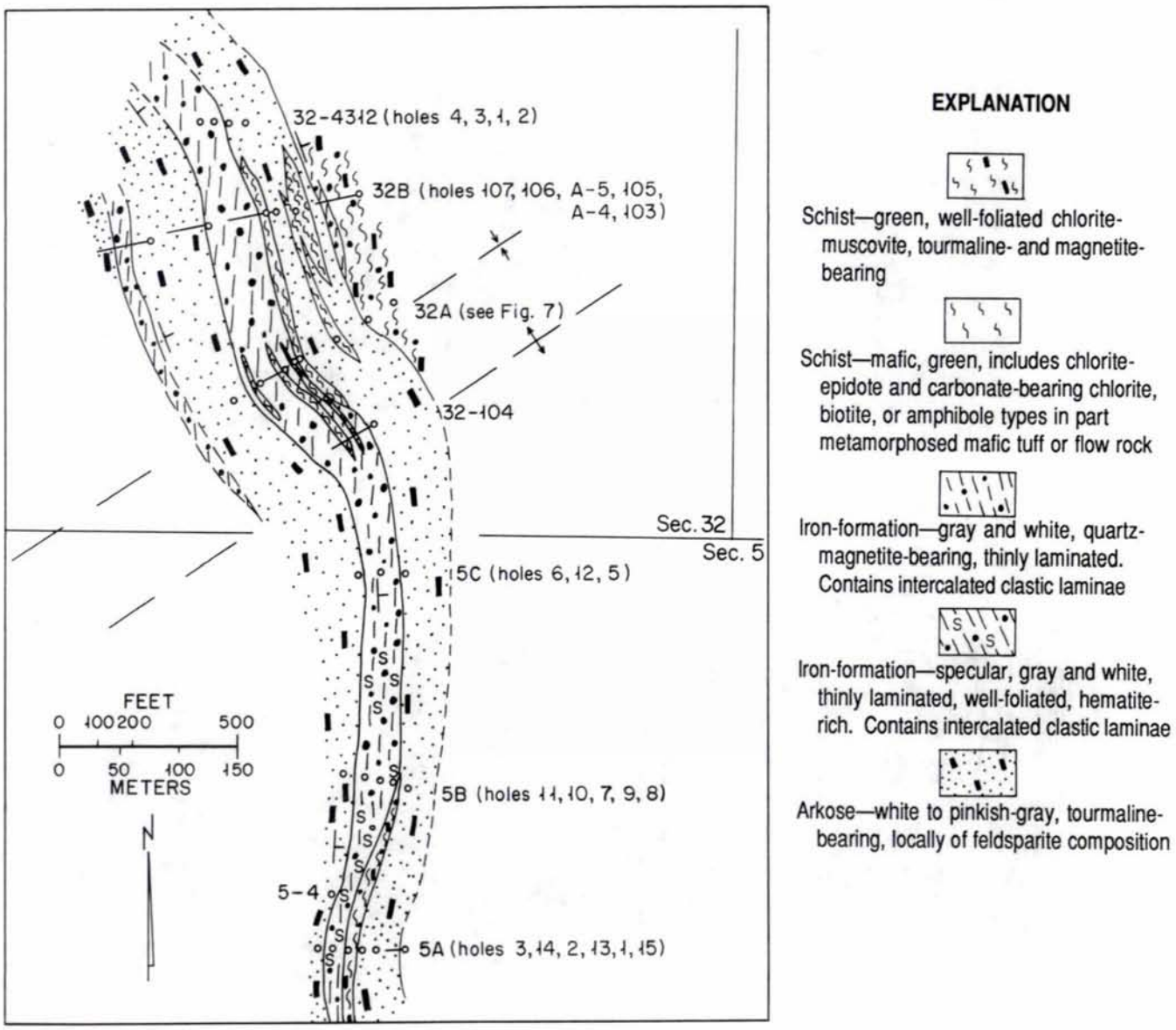

Figure 6. Subcrop map of Philbrook sequence, showing relative locations of drill holes (open circles). Compare with Figures 3 and 5.

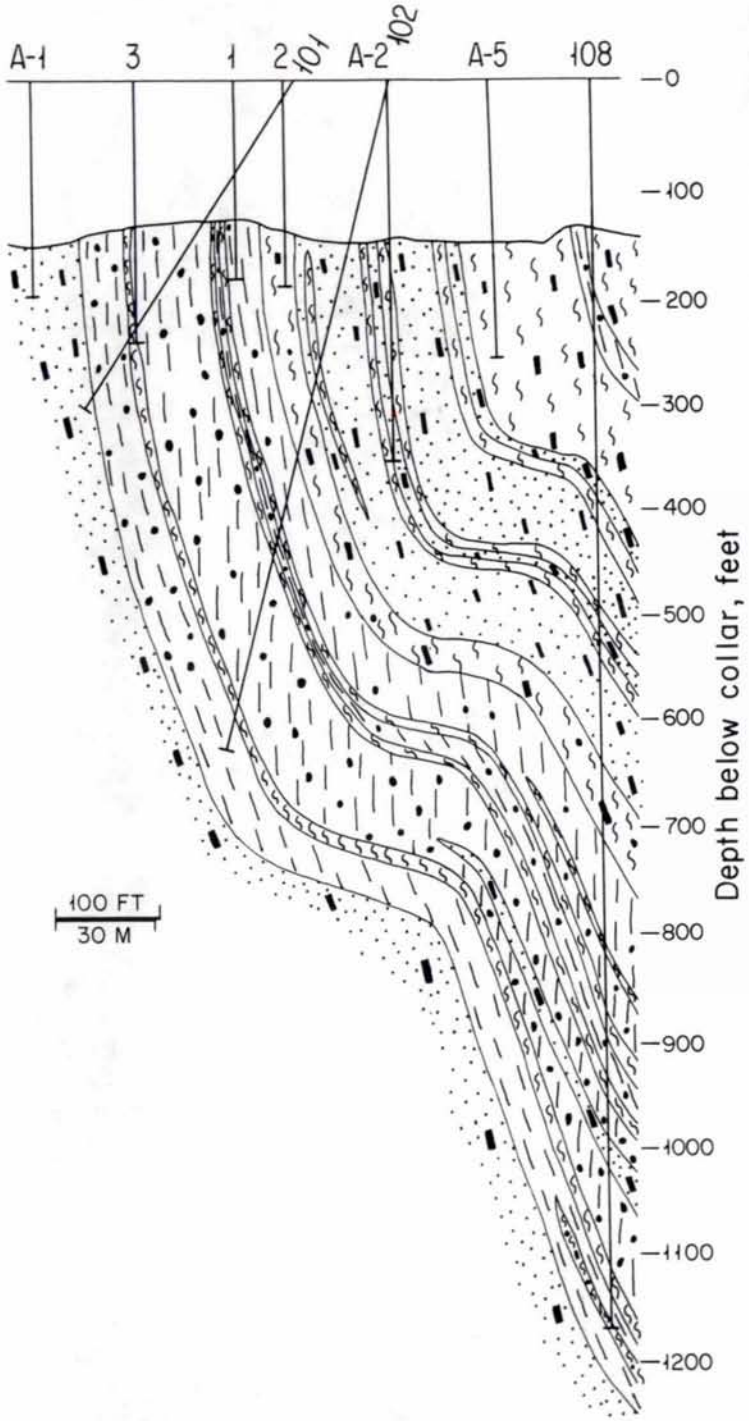

Figure 7. Diagrammatic cross sesction of drill group 32A, facing north. See Figure 6 for drill hole locations and symbols.

units range in thickness from 7 to 35 m. The arkose has a fairly continuous lateral distribution in the area drilled (Figs. 6 and 7). The various schistose units are less well defined, but all seem to occur as scattered lenses, mostly in the iron-formation and the hanging-wall arkose.

Tourmaline occurs most commonly in the arkosic rocks, both as disseminated grains and as tourmaline-rich laminae. Tourmaline also occurs as disseminated grains throughout units of the magnetite-bearing chlorite–muscovite schist.

The stratified rocks of the Philbrook area, like those elsewhere in the Animikie basin, were metamorphosed during the Penokean orogeny. It is not the purpose of this report to discuss the metamorphic history of these rocks, but for the record, the general metamorphic mineral assemblages have been listed in Table 1. These assemblages are indicative of metamorphism under conditions of the upper greenschist or lower amphibolite facies (Turner, 1968).

Table 1. General metamorphic mineral assemblages

Arkose:	quartz–albite–chlorite–biotite–epidote–sericite
Iron-formation:	quartz–magnetite–hematite–chlorite–biotite–epidote–actinolite
Tourmaline- and magnetite-bearing mafic schist:	quartz–albite–chlorite–biotite–sericite
Mafic volcanic rocks:	quartz–chlorite–calcite–epidote–magnetite–ilmenite–sphene–albite
Conglomerates:	quartz–albite–biotite–actinolite–chlorite–epidote

PETROLOGY

Because of the metamorphic overprint, it is not always possible to use conventional sedimentary or igneous rock names. Clues to the original protoliths include relict bedding and rare recognizable rock fragments in the sedimentary rocks, and relict igneous textures in the metavolcanic rocks.

The various rocks of presumed sedimentary derivation were classified in a two-step process, starting with a ternary diagram of end-members quartz + feldspar, phyllosilicates, and opaque iron oxides (Fig. 8); a boundary of 20% modal iron oxides was arbitrarily chosen to separate "iron-formation" from the other sedimentary rocks. Rocks with <20% opaque iron oxide were replotted on a quartz-feldspar-phyllosilicate diagram (Fig. 8b) and named in accordance with the classification scheme of Pettijohn and others (1972). Recognizable rock fragments, although indicative of a sedimentary protolith, are very rare and were omitted from the classification. We assumed that the phyllosilicates muscovite, biotite, and chlorite represent a recrystallized pelitic matrix. We note here that the rocks referred to as arkose could actually be called "feldsparite," inasmuch as albitic plagioclase makes up 40% to 90% of the modal volume.

Iron-Formation

Mappable lithostratigraphic units of the iron-formation, as defined above, range in thickness from 1.5 m to more than 100 m. Typically the rock is grayish green to dark gray, thinly laminated, and magnetic. Individual laminae range in thickness from less than 1 mm to 7 mm. Modal analyses of typical laminae in Table 2 show that individual laminae are defined by different ratios of opaque oxide to quartz. Textural attributes imply that the iron-formation was chemically precipitated. Detrital grains of feldspar (Fig. 9) indicate that some iron-rich laminae are partly terrigenous.

Because of the metamorphic grade, much of the iron-formation consists of a specular schist, which is especially abundant in the southern part of the Philbrook sequence. Although specular hematite is the dominant phase in the schist, the iron-formation to the north consists dominantly of interlocking grains of euhedral magnetite. Minor amounts of the iron silicates epidote, actinolite, biotite, and chlorite occur in both types of iron-formation.

In the quartz-rich laminae the grain size of the quartz decreases as the magnetite content increases. This quartz is presumably recrystallized from an earlier chert precursor. Additional evidence of recrystallization includes micaceous minerals that typically line grain boundaries in mortar-textured quartz aggregates. Although most intercalated laminae of partly terrigenous origin contain only a few percent opaque oxides (Table 2), a few contain as much as 50%. In general, feldspar content increases as magnetite content decreases.

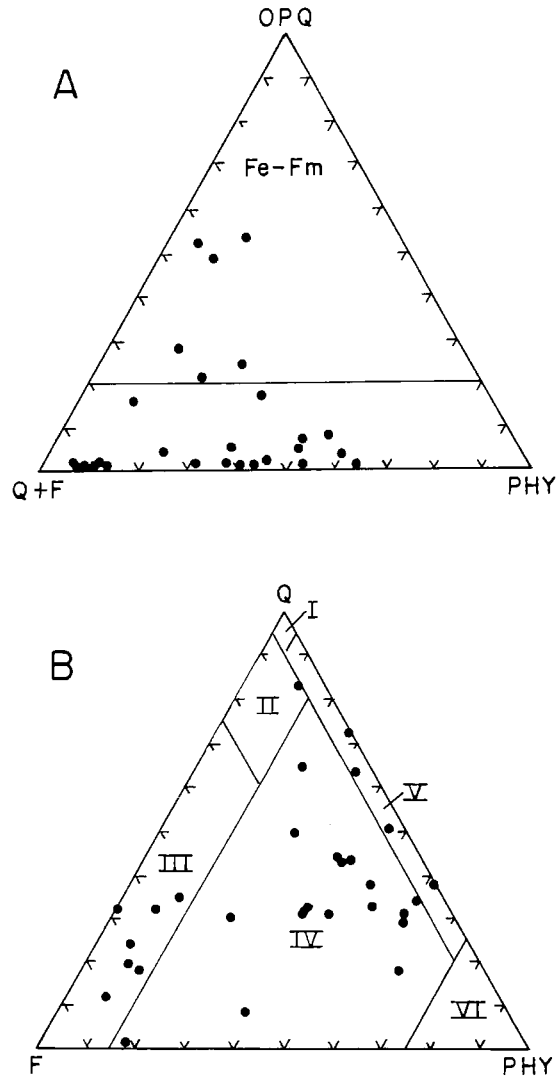

Figure 8. Modal diagrams used to infer protoliths of metasedimentary rocks. OPQ, opaque oxides; Q, quartz; F, feldspar; PHY, phyllosilicates; I, quartz arenite; II, arkose; III, feldspathic arenite; IV, feldspathic graywacke; V, graywacke; and VI, mudstone.

Minor minerals in the iron-formation include apatite of possibly sedimentary derivation. The apatite occurs as thin laminae in several chert-rich laminae, but its origin remains unclear. Skeletal tourmaline occurs locally but is very rare. Typically it is dark gray to semi-opaque, and thus may be more iron-rich than tourmalines in other lithostratigraphic units. Other minor minerals in the iron-formation include epidote and actinolite, which commonly occur along contacts between chert-rich and feldspar-rich laminae. Epidote also

occurs in veins with biotite and chlorite, and other veins are filled with quartz and calcite. The iron-formation also contains chloritized slickensides. Poorly defined shear zones, less than 1 cm thick, contain disseminated blocky pyrite along with chlorite, quartz, and carbonate.

Effects of surface weathering on the iron-formations are generally quite shallow and are expressed by the presence of geothite and limonite after magnetite, hematite, and iron-silicates.

Arkose

Rocks classified as arkose vary in color from light reddish gray to light greenish gray; the greener colors result from slightly more chlorite or biotite. A weak phyllitic sheen is locally imparted by fine-grained sericite. Thin tourmaline-rich laminae are present locally, but are not a prominent feature. Sedimentary structures, such as cross-bedding or grain-size variations, are generally not visible because of incomplete core, and metamorphic overprint has distorted or nearly obliterated original sedimentary grain shapes (Fig. 10). Interstitial areas between framework grains contain chiefly phyllosilicates intermixed with strain-growth quartz and feldspar. This recrystallized quartz and feldspar is so fine that positive identification is impossible, and it is combined as recrystallized quartz plus feldspar in Table 3. However, because this fine quartz-feldspar is a product of recrystallization of the framework grains, the phyllosilicate minerals are classified as recrystallized matrix, and thus 50% to 90% of a typical arkose consists of framework grains of either quartz or feldspar. Feldspar : quartz ratios in distinguishable grains range from 1.5:1 to 9:1, and average approximately 3:1 in the studied samples.

Feldspar grains range in size from 0.03 mm to 1.0 mm across. Optical properties and a single probe analysis (Table 4) indicate that much of the feldspar is near end-member albite (An_{05}). Other studies of tourmalinite occurrences (Nesbitt and others, 1984; Beaty and others, 1988) have shown that the rocks surrounding tourmalinites were heavily albitized by hydrothermal processes; similar processes may have occurred near Philbrook. Feldspar alteration to sericite is nearly ubiquitous, ranging from incipient to complete sericitization.

Granoblastic quartz that is similar in grain size to the feldspar composes the remainder of the framework fraction. Larger grains are typically flattened and somewhat recrystallized; smaller grains are considerably recrystallized. Included in the quartz modes of Table 3 are a few weakly or nonundulose, subequant quartz grains. Although border recrystallization has obliterated any primary volcanic grain shapes, the association of this nonundulose quartz with

Table 2. Modal analyses of iron-formation from drill core
[Tr, trace. Analyses from drill hole 102 are bulk composition, cherty lamina, clastic lamina, respectively, of the same sample.]

	Drill hole and depth (in feet)				
	102 (245-250)			108 (1040-1045)	12 (415-420)
Quartz	34	36	24	27	57
Opaques	38	50	15	46	21
Biotite	9	4	33	6	0
Chlorite	Tr	1	1	5	16
Muscovite	Tr	Tr	Tr	0	6
Feldspar	12	1	19	4	0
Matrix	2	3	1	9	0
Epidote	Tr	0	6	3	0
Tourmaline	4	5	0	0	0
Carbonate	0	0	0	0	1
Sphene	0	0	0	Tr	Tr
Apatite	Tr	Tr	Tr	0	0

Table 3. Modal analyses of arkose from drill core

[Tr, trace. See Table 4 for chemical composition of feldspar; see Table 5 for chemical analyses of samples 3 and 4; see Figure 6 for drill hole locations.]

	Drill hole and depth (in feet)								
	102 (245-250)	103 (485-490)	106 (240)	107 (270)	108 (385-390)	108 (595-600)	A-1 (185-186)	2 (160-165)	11 (155-174)
Quartz	21	13	10	8	Tr	23	20	33	17
Feldspar	37	58	75	75	79	65	42	52	66
Recrystallized Q+F	30	14	5	4	0	3	11	3	5
Biotite	3	5	2	0	2	Tr	0	Tr	1
Chlorite	3	0	3	3	15	5	0	6	4
Muscovite	Tr	6	2	9	0	1	11	5	4
Opaques	Tr	1	0	Tr	2	Tr	0	2	0
Carbonate	1	3	0	Tr	0	1	0	Tr	0
Epidote	3	0	2	Tr	1	0	2	Tr	3
Tourmaline	Tr	Tr	Tr	Tr	0	Tr	15	0	Tr
Sphene	Tr	Tr	Tr	0	0	Tr	0	Tr	Tr
Apatite	0	0	Tr	0	Tr	0	0	0	Tr

strongly zoned oligoclase(?) indicates a possibly volcanic source for the sediments.

Chlorite and biotite compose as much as 6% of a typical arkose, and blocky magnetite and pyrite as much as 2%. Other minerals present in trace amounts include sphene, calcite, epidote, apatite, and slightly rounded prismatic detrital zircon.

Sparse tourmaline-rich laminae contain as much as 50% brown to green pleochroic tourmaline. The tourmaline commonly occurs either as disseminated grains with a prismatic habit (Fig. 11) or as closely packed and intergrown grains (Fig. 12) in discrete laminae. The tourmaline-rich laminae typically contain epidote and heavily sericitized feldspar.

Whole rock analyses (Table 5) confirm the strongly albitic (Na_2O) character of the arkoses, relative to CaO and K_2O. Compared to an average arkose (Pettijohn and others, 1972, p. 60), the "feldsparite" of the Philbrook area contains 4 to 5 times more Na_2O, and less than half as much CaO and K_2O.

Table 4. Chemical composition from microprobe analysis of framework feldspar from arkose

[Drill hole A-1, 175 ft. depth. Sample P19-T175]

SiO_2	65.79
Al_2O_3	18.11
Na_2O	10.67
CaO	1.22
K_2O	0.18
FeO	0.00
Sum	95.98
Number of atoms based on 8 O	
Si	3.00
Al	0.97
Na	0.94
Ca	0.06
K	0.01
Fe	0.00

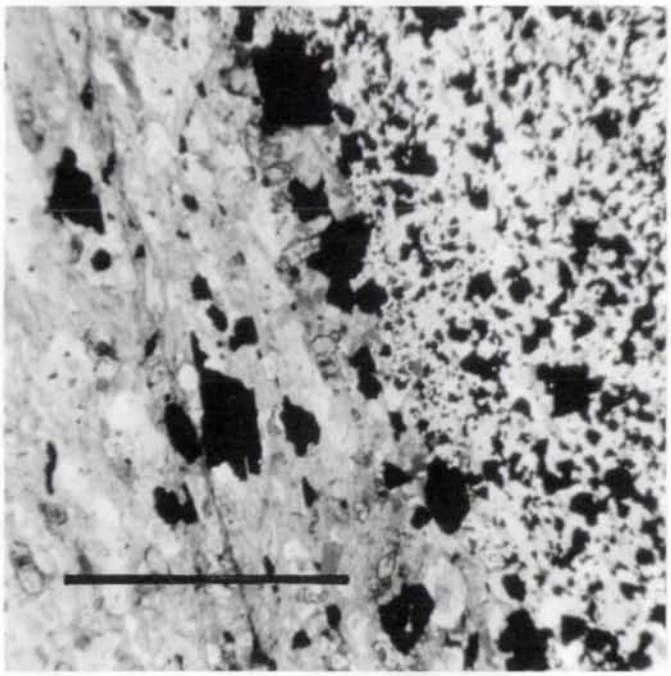

Figure 9. Typical iron-formation showing clastic-dominated lamina (left) and cherty lamina (right). Bar scale 1 mm; plane light. DDH 103 at 410-foot depth.

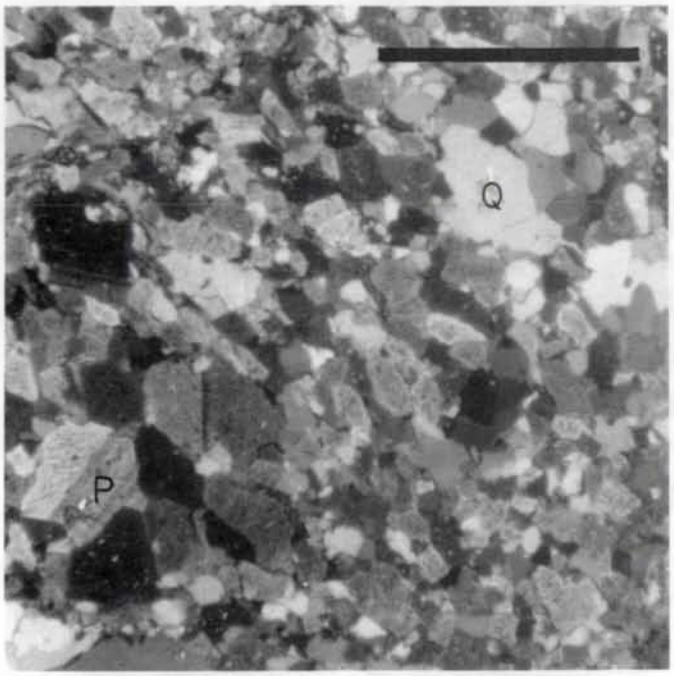

Figure 10. Typical framework constituents in arkose—quartz (Q) and plagioclase (P). Bar scale 1 mm; partially crossed nicols. DDH 108 at depth 595-600 feet.

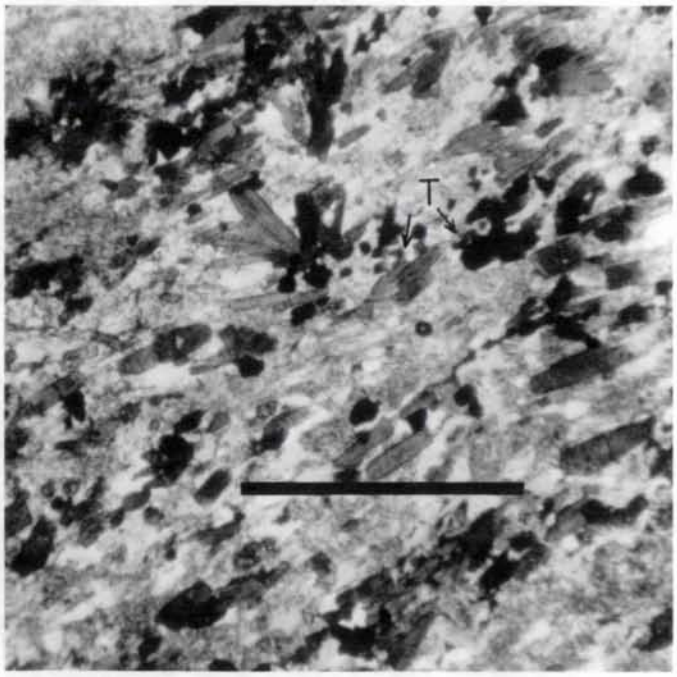

Figure 11. Disseminated brown tourmaline crystals (arrows) in arkose. Bar scale 1 mm; plane light. DDH A-1 at depth 175-176 feet.

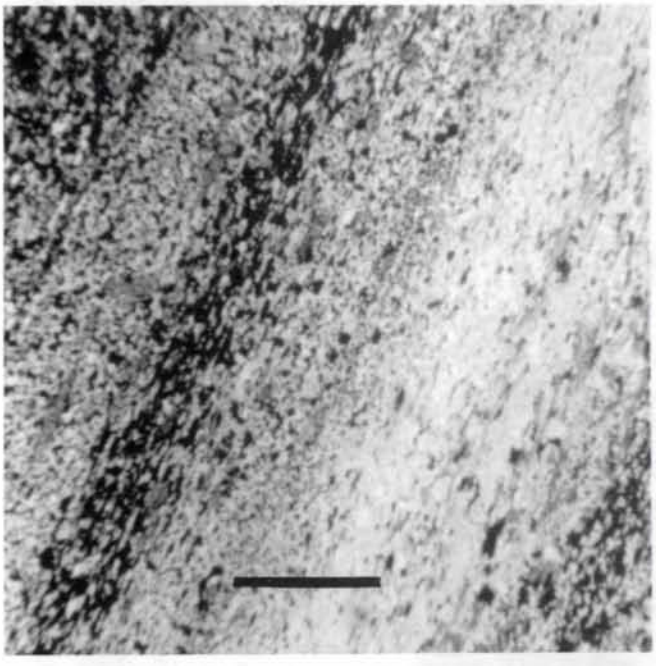

Figure 12. Tourmalinite laminae (black) in arkose. Bar scale 1 mm; plane light. DDH 105 at depth 255-260 feet.

Table 5. Whole rock chemical analyses of arkose, chlorite–muscovite schist, and metabasalt

[Sample numbers correspond to drill hole and depth in feet; see Figure 6 for locations. N/A, not analysed.]

	103-550 arkose	106-240 arkose	107-270 arkose	103-250 schist[1]	108-1147 metabasalt[2]
			Weight percent		
SiO_2	72.40	66.80	63.60	58.70	48.40
TiO_2	0.15	0.16	0.14	0.63	1.23
Al_2O_3	15.30	18.50	19.40	17.10	13.60
Fe_2O_3	<0.10	0.99	0.59	3.50	N/A
FeO	2.05	1.26	1.69	6.70	N/A
MnO	0.03	0.19	0.16	0.06	0.15
MgO	0.84	0.94	1.06	3.82	8.03
CaO	1.36	1.93	1.14	0.81	5.33
Na_2O	6.60	7.06	7.46	1.11	0.26
K_2O	0.40	0.85	1.79	3.47	2.88
P_2O_5	0.04	0.05	0.05	0.18	0.14
Sum	99.17	98.73	97.08	96.08	94.22
Fe_2O_3T	2.26	2.39	2.47	10.90	14.20
			Parts per million		
Be	1	1	2	2	1
Sc	3	3	3	20	53
V	12	17	24	142	390
Cr	7	4	6	158	4
Co	4	5	2	26	61
Ni	8	6	5	89	6
Cu	10	7	5	39	53
Zn	37	38	30	90	150
Rb	8	20	55	117	7
Sr	380	510	372	121	400
Y	4	3	3	17	45
Zr	101	80	80	128	123
Ba	104	339	483	870	520

[1]Chlorite–muscovite schist containing sericite fragments; see Table 6 for modal analysis.

[2]Metabasalt with well-preserved igneous texture; see Table 6 for modal analysis.

Magnetite-Bearing Chlorite–Muscovite Schist

Magnetite-bearing chlorite–muscovite schist typically occurs as a dark-green, fine- to medium-grained, laminated rock unit in the uppermost part of the Philbrook sequence. The schist generally overlies arkose except in the northern part of the area, where an iron-formation intervenes (Fig. 6). The schist also contains layers, generally less than 1 cm thick, of laminated iron-formation. These layers are distributed throughout the schistose interval, but are most abundant in the upper part and in the lower gradational contact with the underlying iron-formation. As in the main iron-formation units, individual laminae are defined by variable ratios of oxides to quartz and contain very little detrital material. The magnetite in the layers is blocky and euhedral and up to 0.1 mm across. However near contacts between iron-rich and detrital-rich layers, magnetite octahedra are typically coarser, up to 0.5 mm across. Chlorite typically is present in the iron-rich layers, and tourmaline locally is concentrated in them.

Representative modes of the schist are given in Table 6. Intergrown chlorite and muscovite account for 15% to 20% of the schist and define the schistosity. Porphyroblasts 1 cm to 5 cm in diameter of chlorite and muscovite are common; the latter are commonly broken and healed with chlorite and granoblastic quartz. Quartz is recrystallized and granoblastic, and the feldspar is moderately to heavily sericitized. White sericitized rock fragments—possibly heavily altered feldspar crystals—as long as 3 cm occur locally and are folded and elongated parallel to foliation (Fig. 13). The presence of sphene and magnetite intergrown with chlorite indicates possible retrograde metamorphism of biotite (Heinrich, 1965, p. 302). Epidote occurs most commonly in chlorite–epidote veinlets. The epidote crystals are euhedral, and contain an allanite core with as many as six overgrowth rims of epidote, which indicate recurring conditions favorable for crystal growth. A whole rock chemical analysis of the schist containing sericite fragments is given in Table 5.

Small amounts of pink to dark-bluish-green pleochroic tourmaline, typically having thin light-green overgrowths, are ubiquitous in this schist. Individual grains are as long as 6 mm and are typically elongated parallel to the foliation (Fig. 14).

Table 6. Modal analyses of magnetite- and tourmaline-bearing chlorite–muscovite schist from drill core

	Drill hole and depth (in feet)				
	103[1] (250)	108 (315-320)	108 (333-360)	108 (350-355)	108 (1165-1170)
Quartz	37	27	30	29	47
Feldspar	12	23	5	13	3
Matrix	0	7	Tr	1	1
Biotite	9	2	13	1	0
Chlorite	27	28	18	23	21
Muscovite	14	5	22	22	22
Opaques	1	5	8	5	2
Carbonate	0	0	0	0	Tr
Epidote	Tr	2	4	4	3
Tourmaline	Tr	Tr	1	2	1
Sphene	1	2	1	1	1
Apatite	Tr	Tr	Tr	Tr	0

[1]See Table 5 for whole-rock chemical analysis of sample.

Mafic Schists

Several varieties of mafic schist are present within the stratigraphic column. These schists are generally distinguished from the more ubiquitous chlorite–muscovite schist by appreciable quantities of carbonate and sulfides and less magnetite (Table 7). Some protoliths are unidentifiable, but some are obviously sedimentary or igneous in origin.

Quartz–Chlorite–Epidote Schist

Stratiform units, typically less than 10 m thick, of calcite-bearing quartz–chlorite–epidote schist occur throughout the stratigraphic sequence and are associated with all of the major rock types. Primary textures are vague, but locally, well-preserved features, particularly a fabric formed by 30% to 40% fresh, tabular feldspar (Fig. 15), imply an igneous protolith. Aggregates of granoblastic quartz comprise 17-23% of the volume and are dispersed throughout the rock. The primary ferromagnesian minerals have been replaced by fine-grained aggregates of chlorite (20-30%), epidote (4-35%), sphene (2-5%), and calcite (3-15%). In extensively altered samples, aggregates of granular epidote are pseudomorphic after feldspar, which is completely obliterated. Consequently, alteration has led to samples which consist nearly entirely of epidote, quartz, and chlorite. Magnetite occurs as embayed or skeletal and ladder-shaped grains and is more or less randomly distributed through the rock.

A whole rock chemical analysis of a sample having a well-preserved igneous texture is given in Table 5. According to the criteria of Irvine and Baragar (1971), this rock would be classified as a tholeiitic basalt. However, the extensive alteration of even this sample implies that any classification based on chemistry should be considered tentative. Nonetheless the textural attributes of the least altered samples, their inferred chemical compositions, and their general stratigraphic occurrence (Figs. 6 and 7) imply that these schistose units originated either as flows or as high-level sills.

Calcite-Bearing Chlorite, Biotite, and Amphibole Schists

These schists are streaky dark green and white, well foliated, and fine to medium grained. They occur as thin units throughout the stratigraphic sequence, but typically are associated with iron-formation. They show textural and compositional similarities, and are probably of similar protolith. Typical examples of this category of schists contain dark-green pleochroic hornblende (as much as 44%), biotite (6% to 53%), chlorite (1% to 27%), quartz (1% to 25%), and albite (10% to 37%). The coarser grained samples typically contain more amphibole and consequently have a darker color.

All of these schists contain albitic feldspar grains which have rounded, indistinct borders due to infringing micas and amphiboles. The feldspar ranges from clean and colorless grains to grains having cores that are altered to biotite and calcite. Rare blocky grains show a perthitic type of texture, presumably due to incomplete albitization. Calcite is most abundant in the more chlorite-rich schists, and occurs in irregular masses and in thin veinlets. Chlorite content, which increases as amphibole content decreases, occurs as folia that bend around feldspar grains parallel to foliation, and in pressure shadows behind pyrite cubes, perpendicular to foliation. Quartz is mostly recrystallized, but rare grains as large as 1 mm are nonundulose and possibly of volcanic origin. Other minerals include trace amounts of epidote, sphene, garnet, and pyrite.

TOURMALINE IN THE PHILBROOK SEQUENCE

As much as 2% by modal volume (Table 6) of the magnetite-bearing chlorite–muscovite schist consists of brownish-orange to dark-bluish-green pleochroic tourmaline. The mineral is more or less ubiquitously distributed throughout the schist, but at several horizons it defines thin laminae (Fig. 14) that are accompanied by appreciable quantities of magnetite. Much of the tourmaline occurs as euhedral to subhedral prismatic crystals 1 to 3 mm in length. The larger grains are for the most part discrete, whereas the smaller grains commonly are included within muscovite poikiloblasts. Regardless of size, the grains have a thick and blocky habit, dark-colored cores, and light-green overgrowths. The cores contain small inclusions of magnetite and quartz. The grain size, habit, and occurrence as inclusions imply a metamorphic origin for this tourmaline. If so, the cores may be the vestiges of a pre-metamorphic precursor.

A few tourmaline grains in the arkosic rocks have attributes like those in the schistose rocks. However here most of the tourmaline is dominated by a distinct greenish-brown to semi-opaque variety which is much richer in magnesium and closer to the dravite end-member than the bluish-green variety in the chloritic schist. This greenish-brown variety lacks a distinctive core but does have thin light-brown overgrowths that tend to cap crystal termini.

Tourmaline comprises as much as 15% of the modal volume of the arkose. Typically the tourmaline is more or less diffusely scattered throughout the rock (Fig. 11). However, the arkosic units also contain both sharply and diffusely bounded laminae, 0.5 mm to 1.5 mm thick, that contain as much as 50% tourmaline (Fig. 12). Generally, individual grains in the tourmalinite laminae are smaller than those that are diffusely scattered throughout arkosic beds. The tourmaline-rich laminae seem to have developed in response to primary sedimentary processes.

Table 7. Modal analyses of various mafic schists from drill core

	Drill hole and depth (in feet)										
	108 (1145)[1]	108 (1055-160)	105 (515-520)	104 (410-415)	104 (300-305)	103 (385-400)	101 (276-281)	15 (355-360)	15 (270-300)	10 (255-260)	8 (150-155)
Quartz	17	15	*	40	23	Tr	21	25	20	12	7
Feldspar	29	51	*	13	4	27	Tr	10	18	11	43
Matrix	Tr	5	0	5	4	2	0	0	2	6	1
Biotite	1	10	37	20	1	22	5	23	21	53	3
Chlorite	28	1	3	0	35	Tr	30	27	4	0	20
Muscovite	Tr	0	1	20	Tr	0	0	0	0	10	0
Opaques	5	15	0	1	6	Tr	2	Tr	20	1	1
Carbonate	15	2	0	Tr	3	Tr	3	4	7	3	20
Epidote	4	1	9	Tr	20	2	34	8	7	3	1
Tourmaline	0	0	0	0	1	0	0	0	Tr	0	0
Sphene	2	0	0	Tr	2	1	5	3	Tr	1	4
Apatite	0	Tr	0	0	0	Tr	0	Tr	1	Tr	0
Garnet	0	0	0	0	0	0	0	0	0	0	Tr
Amphibole	0	0	0	0	0	44	0	0	0	3	0

*Total quartz + feldspar = 61.

[1]See Table 5 for whole-rock chemical analysis of sample.

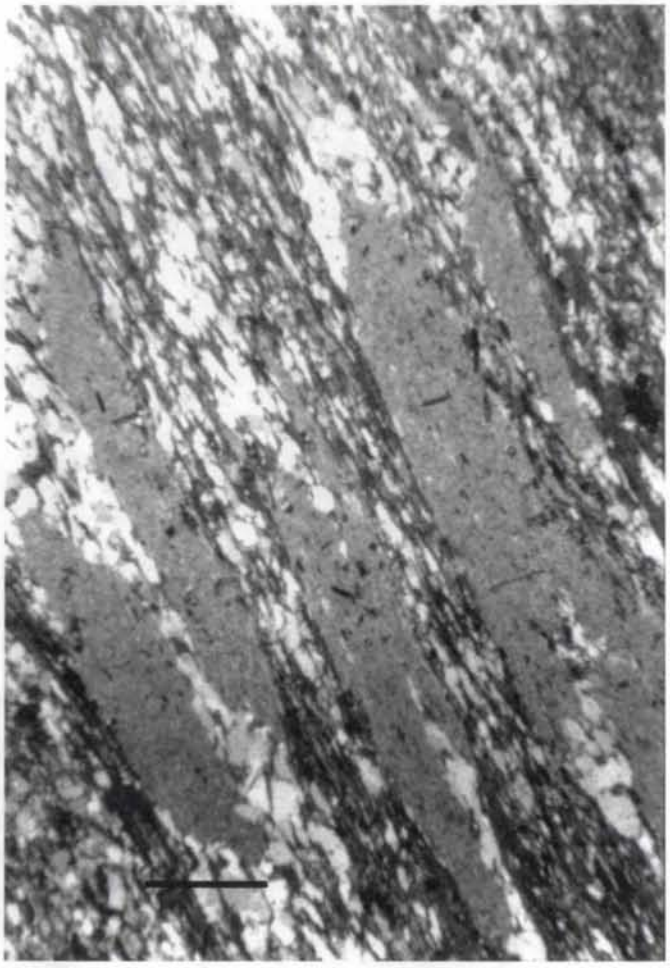

Figure 13. Sericite-rich, flattened fragments, probably from a felsic volcanic protolith, from upper tourmaline-bearing chloritic schist. Bar scale 1 mm; plane light.

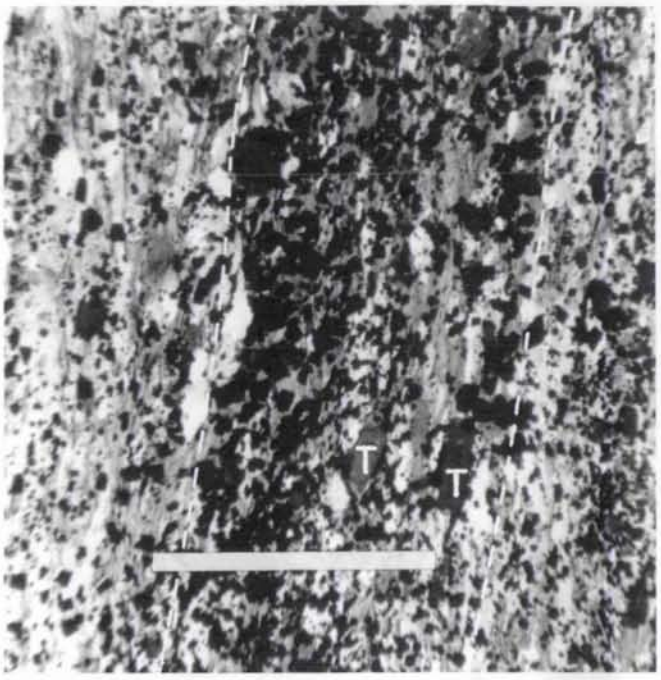

Figure 14. Tourmaline (T) and magnetite bedding concentration (inside dashed lines) in chlorite–muscovite schist. Bar scale 1 mm; plane light. DDH 108 at depth 365-370 feet.

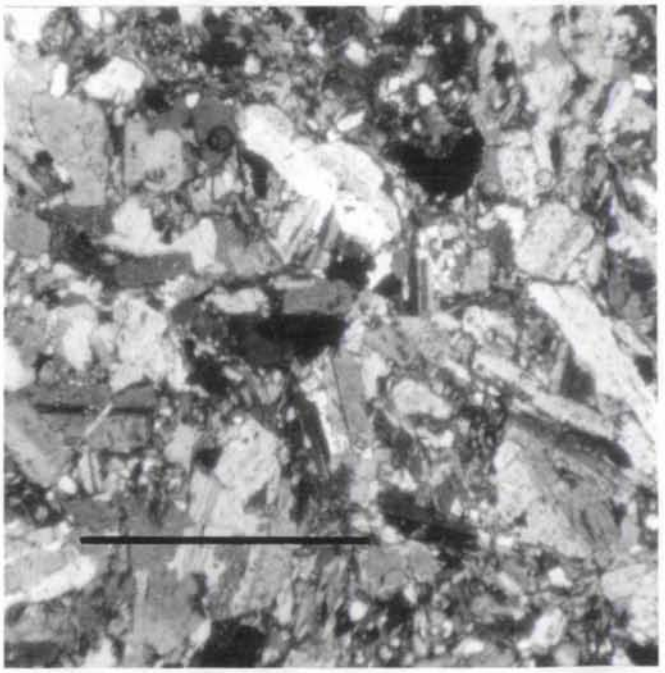

Figure 15. Photomicrograph showing well-preserved texture of metabasalt from chlorite-epidote schist. Bar scale 1 mm; crossed nicols. DDH 108 at depth 1145 feet.

Chemical Analyses of Tourmaline

A limited amount of chemical data were obtained to further characterize the several kinds of tourmaline observed in the Philbrook sequence. A single quantitative chemical analysis (Table 8, sample 11) was obtained from the bluish-green variety typical of the magnetite-bearing chlorite–muscovite schist. Additional major-element data were obtained by electron microprobe for both this variety and the greenish-brown variety typically found in the arkosic units (Table 8). Although the analysis of tourmalines by electron microprobe techniques can be plagued by a variety of problems (Ethier and Campbell, 1977), we obtained consistent results and thus the differences observed between samples probably are real rather than analytical. To further reduce analytical uncertainty, percentages of the oxide ratios $Na_2O/(Na_2O+K_2O+CaO)$ and $FeO/(FeO+MnO+MgO)$ were used to characterize the tourmalines rather than the oxide values themselves (Ethier and Campbell, 1977; Taylor and Slack, 1984). This approach and the classification scheme of Henry and Guidotti (1985) indicate that the tourmalines from the Philbrook area have a composition between that of dravite (the magnesian end-member), and that of schorl (the iron end-member). The greenish-brown tourmalines also contain appreciable calcium and consequently plot slightly towards the end-member defined by uvite (Fig. 16).

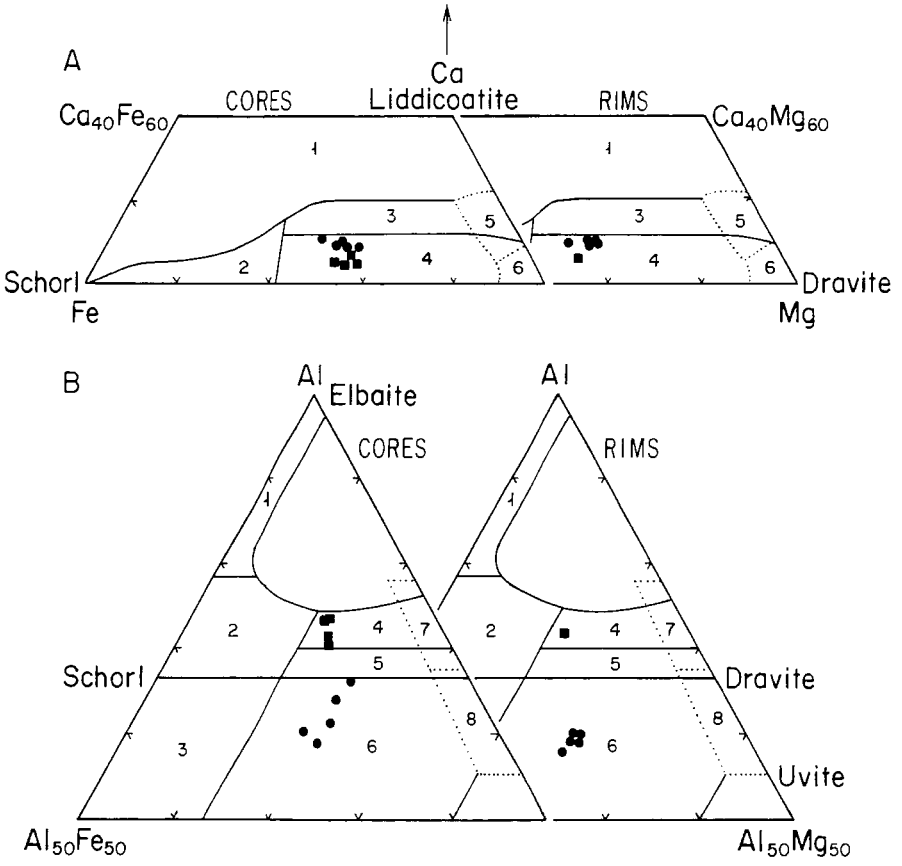

Figure 16. Tourmaline rim and core compositions from Philbrook sequence. Modified from Henry and Guidotti (1985).
(A) Ca-Fe-Mg diagram. Fe is total iron as FeO. Squares, tourmaline from magnetite- and tourmaline-bearing schist; dots, tourmaline from arkosic rocks. Fields as in B.
(B) Al-Fe-Mg diagram. The fields represent: (1) Li-rich granitic pegmatites and aplites; (2) Li-poor granitic pegmatites and aplites; (3) Fe+3-rich quartz-tourmaline rocks (hydrothermally altered granites); (4) metapelites and metapsammites coexisting with an Al-saturating phase; (5) metapelites and metapsammites not coexisting with an Al-saturating phase; (6) Fe+3-rich quartz-tourmaline rocks, calc-silicate rocks, and metapelites; (7) low-Ca meta-ultramafics and Cr, V-rich metasediments; and (8) metacarbonates and metapyroxenites.

Table 8. Chemical compositions of tourmaline from tourmaline- and magnetite-bearing chlorite–muscovite schist (1-3, 11), and from arkose (4-10)

[Samples 1-10 from electron microprobe; sample 11 from wet chemical analysis of a tourmaline concentrate. Samples 1a, 1b, etc., rechecks of same approximate probe point. N/A, not analysed for; results in weight percent; trace elements in ppm.]

	1	1a	1b	1c	2	3	4	5	5a	6	7	8	9	10	10a	11
SiO_2	34.23	33.82	32.32	33.34	33.91	34.16	34.55	34.41	30.56	30.51	30.30	31.38	30.65	32.15	29.98	35.40
Al_2O_3	33.20	30.68	34.23	30.78	34.59	33.76	22.71	21.75	24.43	25.44	24.88	27.63	24.90	28.24	23.37	29.20
Na_2O	2.16	2.16	1.91	2.00	2.09	2.23	1.81	1.82	1.94	1.92	1.93	2.17	1.96	2.33	2.00	2.01
CaO	0.81	0.79	0.74	0.80	0.90	0.77	2.04	2.02	1.91	2.01	2.06	1.62	2.05	1.28	1.95	1.04
K_2O	0.09	0.09	0.09	0.08	0.10	0.10	0.14	0.14	0.15	0.18	0.16	0.13	0.15	0.10	0.15	0.12
FeO	7.78	7.79	6.99	7.24	8.07	8.17	10.96	11.36	10.07	10.37	10.55	9.69	10.49	8.16	10.33	9.73
MgO	5.78	5.72	5.32	5.66	5.46	5.66	6.37	6.77	7.13	7.24	7.48	6.83	7.44	7.10	7.22	5.60
MnO	N/A	N/A	N/A	N/A	N/A	N/A	N/A	N/A	N/A	N/A	N/A	N/A	N/A	N/A	N/A	0.02
TiO_2	N/A	N/A	N/A	N/A	N/A	N/A	N/A	N/A	N/A	N/A	N/A	N/A	N/A	N/A	N/A	0.55
P_2O_5	N/A	N/A	N/A	N/A	N/A	N/A	N/A	N/A	N/A	N/A	N/A	N/A	N/A	N/A	N/A	0.16
Total	84.05	81.05	81.60	79.90	85.12	84.85	78.58	78.27	76.19	77.67	77.36	79.45	77.64	79.37	75.00	83.83
	Number of ions based on 20 oxygen															ppm
Si	4.71	4.83	4.56	4.82	4.62	4.67	5.24	5.26	4.80	4.71	4.71	4.67	4.74	4.75	4.81	Sr 316
Al	5.39	5.17	5.70	5.24	5.55	5.44	4.06	3.92	4.52	4.63	4.55	4.88	4.55	4.92	4.41	Ba 23
Na	0.58	0.60	0.52	0.56	0.55	0.60	0.53	0.54	0.59	0.58	0.58	0.63	0.59	0.67	0.62	Be 1
Ca	0.12	0.12	0.11	0.12	0.13	0.11	0.33	0.33	0.32	0.33	0.34	0.26	0.34	0.20	0.33	Zn 98
K	0.02	0.02	0.02	0.02	0.12	0.02	0.03	0.03	0.03	0.04	0.03	0.03	0.03	0.02	0.03	Cu 302
																Sc 19
																Co 1
Fe	0.90	0.93	0.83	0.88	0.92	0.93	1.39	1.45	1.32	1.34	1.37	1.22	1.36	1.01	1.38	Ni 110
Mg	1.19	1.22	1.12	1.22	1.11	1.15	1.44	1.54	1.67	1.67	1.73	1.53	1.72	1.56	1.73	Cr 1
																V 182
																Zr 91
																Y 7

1 Core, dark-bluish-green tourmaline, DDH 108, 355-ft. depth.
2 Midway between core and rim, same crystal.
3 Rim, same crystal.
4 Midway between core and rim, greenish-brown tourmaline,DH A-1, 175-ft. depth.
5 Rim, same crystal.
6 Core, greenish-brown tourmaline, DDH A-1, 175-ft. depth.
7 Rim, same crystal.
8 Core, greenish-brown tourmaline, DDH A-1, 175-ft. depth.
9 Rim, same crystal.
10 Core, greenish-brown tourmaline, DDH A-1, 175-ft. depth.
11 Concentrate of dark-bluish-green (microscopic) or brownish-black (macroscopic) tourmaline, DDH 108, upper part of drill core; trace elements in ppm.

Chemical studies in general have shown that tourmalines formed in a stratiform setting are distinctly different from those found in an igneous environment, especially with regard to FeO/(FeO+MgO) ratios (Ethier and Campbell, 1977; Taylor and Slack, 1984; Appel, 1984; Plimer, 1986, 1987; Beaty and others, 1988; Plimer and Lees, 1988). Tourmaline from stratiform tourmalinites is typically richer in Mg, having FeO/(FeO+MgO) values of 0.21 to 0.60, compared to igneous tourmaline, which is typically Fe-rich, having FeO/(FeO+MgO) values approximately 0.85. The stratiform tourmaline from Roseberry is considerably different from those reported elsewhere. In addition, several other characteristic major- and minor-element attributes, as summarized in Table 9, also distinguish stratiform tourmalines from igneous tourmalines.

As Table 9 shows, the FeO/(FeO+MnO+MgO) ratio for the average Philbrook tourmaline is slightly higher than that of the average stratiform tourmaline (Figs. 17 and 18), but close to the values given by Plimer (1986) for tourmaline from the Golden Dyke Dome deposit in Australia. However, the barren tourmalinites of Trestle Creek, Idaho, in the Belt-Purcell Supergroup (in which the Sullivan deposit also occurs), show a slightly higher FeO/(FeO+MnO+MgO) ratio than tourmaline from mineralized tourmalinites in the Sullivan orebody (Beaty and others, 1988). Also note (Table 9; Fig. 18) that the non-mineralized host rocks for the Sullivan orebody have an average FeO/(FeO+MnO+MgO) ratio similar to Philbrook. This suggests that the tourmalinites of this study are also barren, but it does not preclude the possibility of mineralization elsewhere in the sequence.

ECONOMIC SIGNIFICANCE OF THE TOURMALINITES

Tourmaline is a common mineral which occurs in a variety of geologic environments. Bedded, stratiform, tourmaline-rich rocks (tourmalinites) are typically associated with stratabound massive sulfide deposits containing copper, lead, zinc, and gold (see references in Table 10). Thus the presence of tourmalinites may be indicative of geologic environments suitable for the development of base-metal sulfide deposits.

Tourmalinites commonly occur in Proterozoic or Early Paleozoic rift basins where the sedimentary fill is dominantly argillite or sandstone. Other associated rocks may include silicic volcanic rocks, oxide-facies iron-formation, mafic metavolcanic rocks, and calc-silicate schists. Evidence pointing to sedimentary origin for the tourmalinites includes fine-scale (<1 mm) laminae which typically exhibit graded bedding, cross-laminated bedding, slump and flame structures, and rip-up clasts of tourmalinite in a tourmaline-free matrix (Slack and others, 1984; Ethier and Campbell, 1977; Appel, 1984; Nesbitt and others, 1984).

The amount of tourmaline that can form in any sedimentary environment is controlled by how much boron is present. In general, boron is concentrated into a sedimentary system either by hypersaline conditions in a sabkha-type environment or by submarine exhalative processes in and around fault-controlled vent systems (Ethier and Campbell, 1977; Appel, 1984; Nesbitt and others, 1984; Slack and others, 1984; Taylor and Slack, 1984; Plimer, 1986; Plimer and Lees, 1988).

Textural relationships, chemical zonation within tourmaline, and observed mineral assemblages, led Taylor and Slack (1984) to suggest that the tourmaline formed initially in a diagenetic environment and was subsequently modified by metamorphic processes. Plimer (1986) has suggested that the abundant clay in argillaceous sediments is a likely source of boron, as clay minerals are already enriched in boron relative to other minerals. Hydrothermal waters, derived either from circulating seawaters or connate water, strip the argillaceous sediments of boron and metals and redeposit them at exhalative vents. Anomalously high heat flow associated with rifting and diabasic sills acts as the driving force for the hydrothermal systems. Similarly, Nesbitt and others (1984) have shown with oxygen isotopes that the tourmalinites at the Sullivan mine in British Columbia formed from boron that was carried by low-temperature (<110°C) connate fluids that were vented and deposited either at the sediment-water interface or in very shallow beds that had appreciable porosity and permeability. Venting was accomplished during sedimentation by loading and dewatering along conduits localized by a deep synsedimentary fracture system. Younger, hotter (150°C) Pb-Zn-Fe-bearing fluids utilized the same fracture system to produce stratiform sulfide deposits. The same fracture system also was utilized by a final hydrothermal event (250°C) that altered the tourmalinite and ore, and produced albite-chlorite assemblages in the sedimentary rocks on the hanging wall. Plimer and Lees (1988) suggest that tourmaline was deposited in exhalites which formed slightly after and distal to the orebodies in the Roseberry Zn-Pb-Cu-Ag-Au deposit in Western Tasmania, Australia. In any case, tourmaline formation is commonly an integral part of the ore-forming process.

The fact that the tourmalinites in the Philbrook sequence resemble those associated with massive sulfide deposits implies that an exhalative model like that proposed for the Sullivan and similar deposits might also be applicable in the Philbrook area and possibly in other parts of the Animikie basin.

Other geologic factors bearing on the possible presence of a stratiform base-metal sulfide deposit in the Philbrook area are: (1) association with arkosic sediments, (2) fairly abrupt changes in rock types, which in turn imply tectonic activity within the deposystem, and (3) the presence of iron-formations, suggestive of exhalative processes. These factors collectively imply deposition in a restricted basin bounded by faults that could also serve as conduits for migrating fluids. Extensive albitization and the presence of other hydrothermal assemblages argue for the existence of such fluids.

Table 9. Chemical characteristics of tourmaline from the Philbrook area compared to tourmaline associated with stratiform, sediment-hosted sulfide deposits and an igneous body

[N/A, not analyzed for]

	Philbrook	Appalachia[1]	Trestle Creek[2]	Golden Dyke Dome[3]	Sullivan orebody[4]	Sullivan host rocks[4]	Roseberry[5]	Igneous[4]
				FeO/(FeO+MnO+MgO)				
Range	0.58-0.61	0.06-0.04	0.46-0.64	0.47-0.58	0.23-0.32	0.45-0.67	0.72-0.88	0.82-0.91
Average	0.59	0.21	0.56	0.53	0.28	0.60	0.83	0.85
				$Na_2O/(Na_2O+K_2O+CaO)$				
Range	0.45-0.49	0.53-0.89	N/A	0.55-0.64	0.33-0.90	0.62-0.73	0.86-0.95	0.87-0.93
Average	0.47	0.63		0.62	0.52	0.70	0.93	0.88
				High in (ppm):				
Cr	193	78	N/A	N/A	N/A	N/A	N/A	N/A
Cu	302	77	N/A	N/A	N/A	N/A	N/A	N/A
V	182	195	N/A	N/A	N/A	N/A	N/A	N/A
				Low in (ppm):				
Mn	179	382	N/A	N/A	N/A	N/A	N/A	N/A

[1]Taylor and Slack, 1984
[2]Beaty and others, 1988
[3]Plimer, 1986
[4]Ethier and Campbell, 1977
[5]Plimer and Lees, 1988

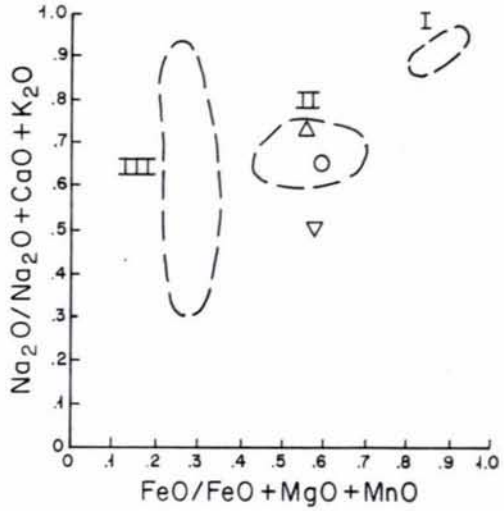

Figure 17. Tourmaline compositions from Philbrook compared to compositions from Sullivan in terms of oxide ratios. III, Sullivan orebody; II, host rocks; and I, a nearby igneous intrusion (modified from Ethier and Campbell, 1977). Circle, wet chemical analysis from Philbrook tourmaline- and magnetite-bearing schist; upright triangle, microprobe composition from same rock; inverted triangle, composition from arkosic rocks.

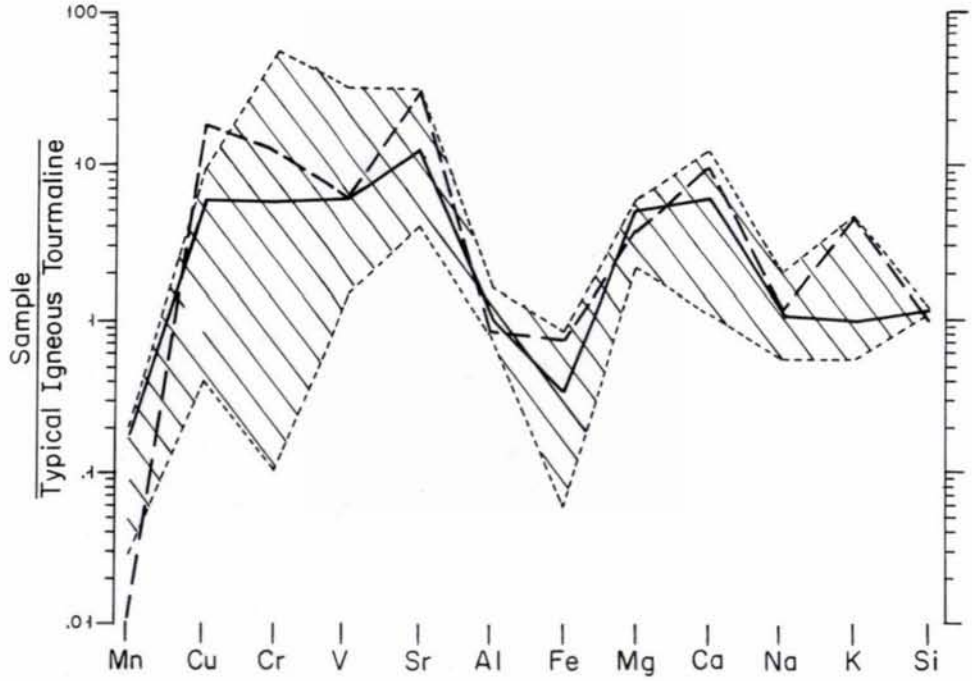

Figure 18. Comparison of Philbrook tourmaline with massive sulfide-related tourmalines from the Appalachian region reported by Taylor and Slack (1984). Ruled area, range of tourmaline associated with massive-sulfide deposits; solid line, average of sulfide-related tourmalines; dashed line, Philbrook tourmaline (Table 8, column 11).

Table 10. Capsule descriptions of geologic associations of tourmaline-bearing sequences

Location	Associated Lithology	Reference
Passagem de Mariana (Brazil)	Quartzite, pelitic schist and phyllite, iron-formation	Fleischer and Routhier, 1973
Elizabeth mine (Vermont)	Quartz-rich schist, calcareous hornblende, tremolite, or phlogopite schist	McKinstry and Mikkola, 1954; Howard, 1969
Ely mine (Vermont)	Quartz-mica schist, amphibolite, quartzite	White and Eric, 1944
Black Hawk mine (Maine)	Quartzite, quartz-mica-chlorite schist, biotite-cordierite schist	LaPierre, 1977; Badawy, 1978
Ore Knob (N. Carolina)	Quartz-mica-plagioclase gneiss, amphibolite	Espenshade, 1963; Kinkel, 1967
Bliekvassli (Norway)	Quartz-mica schist, quartzite, microcline gneiss, amphibolite	Vokes, 1966 (Above references taken from Taylor and Slack, 1984)
Woodcutter's Prospect (Australia)	Shale and dolomite	Roberts, 1973 (cited in Ethier and Campbell, 1977)
South Carolina	Iron-formation, pelitic schist, quartzite, felsic volcaniclastic rocks	Mittwede, 1984
Sullivan (Canada)	Quartz-mica schist, conglomerate (breccia), argillite, arenite	Ethier and Campbell, 1977; Nesbitt and others 1984
Trestle Creek (Idaho)	Siltstone, quartzite, conglomerate	Beaty and others, 1988
Lawrence County (New York)	Feldspathic quartzite, metapelite, tremolite schist, quartz-feldspar-mica granofels, marble	Brown and Ayuso, 1988
Roseberry deposit (Australia)	Metamorphosed felsic volcanic rock	Plimer and Lees, 1988
Golden Dyke Dome (Australia)	Carbonaceous pelitic metasedimentary rocks	Plimer, 1986
Precambrian rift environments	Prograde calc-silicate rocks, amphibolites (associated with tungsten)	Plimer, 1987
Rum Jungle (Australia)	Arenite, magnesite, iron-formation, mafic tuff	Bone, 1988

A PROPOSED GEOLOGIC HISTORY FOR THE PHILBROOK SEQUENCE

As judged from several small outcrops, the Archean basement in the Philbrook area consists dominantly of tonalite, a fairly common Archean rock. The basement also consists in part of metavolcanic rock types typical of the Archean, which occur as clasts in tonalitic conglomerate. Lithologically different quartz-rich conglomerates also crop out in the Philbrook area, but their stratigraphic relationship to the tonalite and tonalitic conglomerate or to the Philbrook sequence is unknown. On the basis of regional considerations, Southwick and others (1988) have suggested that both types of conglomerate occur near the base of the Early Proterozoic Animikie Group, and therefore unconformably overlie both the Archean and the Early Proterozoic Philbrook sequence.

Regardless of their precise stratigraphic position, the conglomerates imply a sedimentary regime involving nearby source areas and fairly high-energy depositional environments. Because of their inferred stratigraphic position beneath the Animikie Group, the metasedimentary rocks of the Philbrook sequence proper are assigned to the Mille Lacs Group (Southwick and others, 1988), a tentative correlation also based in part on lithological similarities to rocks of the Mille Lacs Group that crop out in other parts of the Animikie basin.

Regional considerations indicate that the Philbrook sequence was deposited along the northwestern edge of the Animikie basin. The nature of its contacts with the Archean basement and the overlying Animikie Group is unknown, however, as are the lithic attributes of the Early Proterozoic rocks above and below the stratigraphic interval intersected at Philbrook.

The Philbrook sequence shows two sedimentary cycles—an older cycle trending from arkose to iron-formation, and a younger cycle trending from arkose to graywacke. The first cycle involved a decrease with time in the amount of clastic material being supplied to the basin, culminating in a starved basin in which chemical deposition of the iron-formation took place. In contrast, the second cycle involved a relative increase in the amount of fine-grained muddy material being introduced into the basin. We suggest that the cycles reflect changes in the configuration of the basin, either in response to tectonic processes or simply changes in the geometric properties of the sedimentary fill. The presence of abundant plagioclase, together with a lack of appreciable orthoclase, is consistent with a tonalitic source area like that of the greenstone-granite terrane to the north, rather than the presumably gneissic terrane to the south. The relatively good sorting implies initial deposition in a shallow-water environment and mechanical reworking either in shallow water or with redeposition in deep water by submarine fan processes or by slumping. However, the composition of the source area and subsequent sedimentary processes do not explain the dominance of albitic plagioclase and the extremely high $Na_2O/(K_2O+CaO)$ ratios (Table 5). Therefore, it seems likely that the arkosic sediments were subjected to a period of albitization by hydrothermal processes, which could also account for presence of tourmalinites.

The observations outlined are consistent with the sedimentation models of Meyn and Palonen (1980) and Barrett and Fralick (1985) from well-documented Archean sequences. In those models, sandstone/shale/iron-formation are related to turbidite deposition in a series of submarine fan complexes that migrate in position through time. The graywacke represents deposits formed by through-going currents. In contrast, the arkose represents deposits that were mechanically disaggregated and sorted in temporary upslope basins and were redeposited in a submarine-fan environment. Throughout the depositional history, iron-formations accumulated during periods of quiet clastic sedimentation.

Thin mafic metavolcanic units probably resulted from the upwelling of basaltic material along rift faults, and its intrusion as sills or dikes or extrusion as subaqueous flows. These mafic rocks are particularly abundant in units of iron-formation and in the upper part of the sequence. This suggests that the iron-formation could well have formed by exhalative processes associated with seafloor vents and convection systems that would likely have developed along fracture zones.

The general observation that the tourmaline, either as discrete grains or in tourmalinites, and magnetite, either as discrete grains or in iron-formation, locally occupy the same stratigraphic position implies that the exhalative processes responsible for the iron and silica also were the source of the boron. Therefore it seems likely that periodic pulses of boron-rich fluids from a fracture system were spread across the seafloor as density flows, to be included within thin sedimentary intervals. The boron may also have been concentrated in permeable beds adjacent to the conduits which vented it to the seafloor. Regardless, the boron was available for incorporation into tourmaline under the proper diagenetic and/or metamorphic conditions.

ACKNOWLEDGMENTS

D.L. Southwick and G.B. Morey of the Minnesota Geological Survey provided advice and assistance during the preparation of the study as a Master's thesis at the University of Minnesota–Duluth. R.W. Ojakangas and J.C. Green of the University of Minnesota•Duluth reviewed the manuscript of the thesis. The Minnesota Geological Survey supplied financial assistance for this study, and the Minnesota Department of Natural Resources provided financial assistance for many assays and thin section mounts during thesis preparation.

REFERENCES CITED

Appel, P.W.A., 1984, Tourmaline in the early Archean Isua supracrustal belt, West Greenland: Journal of Geology, v. 92, p. 599-605.

Badawy, A.M., 1978, Sulfide-silicate metamorphism at the Blue Hill copper-zinc mine, Maine: Unpublished Ph.D. dissertation, Boston University, 170 p.

Barrett, T.J., and Fralick, P.W., 1985, Sediment redeposition in Archean iron-formation: Examples from the Beardmore-Geraldton greenstone belt, Ontario: Journal of Sedimentary Petrology, v. 55, p. 205-212.

Beaty, D.W., Hahn, G.A., and Threlkeld, W.E., 1988, Field, isotopic, and chemical constraints of tourmaline-bearing rocks in the Belt-Purcell Supergroup: Genetic constraints and exploration significance for Sullivan-type ore deposits: Canadian Journal of Earth Sciences, v. 25, p. 342-402.

Boerboom, T.J., 1987, Tourmalinites, nelsonites, and related rocks (Early Proterozoic) near Philbrook, Todd County Minnesota: Unpublished M.S. thesis, University of Minnesota–Duluth, 212 p.

Bone, Y., 1988, The geological setting of tourmalinite at Rum Jungle, N.T., Australia: Genetic and economic implications: Mineralium Deposita, v. 23, p. 34-41.

Brown, C.E., and Ayuso, R.A., 1985, Significance of tourmaline-rich rocks in the Grenville complex of St. Lawrence County, New York: Chapter C *of* Contributions to the geology of mineral deposits: U.S. Geological Survey Bulletin 1626, p. C1-C33.

Chandler, V.W., 1984, Aeromagnetic map of Minnesota, total magnetic intensity anomaly and flightline recovery, Motley 7.5-minute quadrangle: Minnesota Geological Survey Open-File Map, scale 1:24,000.

Dacre, C.J., Himmelberg, G.R., and Morey, G.B., 1984, Pre-Penokean igneous and metamorphic rocks, Benton and Stearns Counties, central Minnesota: Minnesota Geological Survey Report of Investigations 31, 16 p.

Espenshade, G.H., 1963, Geology of some copper deposits in North Carolina, Virginia, and Alabama: U.S. Geological Survey Bulletin 1142-I, 50 p.

Ethier, V.G., and Campbell, F.A., 1977, Tourmaline concentrations in Proterozoic sediments of the southern Cordillera of Canada and their economic significance: Canadian Journal of Earth Sciences, v. 14, p. 2348-2363.

Fleischer, R., and Routhier, P., 1973, The "consanguineous" origin of a tourmaline-bearing gold deposit: Passagem de Mariana (Brazil): Economic Geology, v. 68, p. 11-22.

Heinrich, E.W., 1965, Microscopic identification of minerals: McGraw-Hill, 414 p.

Henry, P.J., and Guidotti, C.V., 1985, Tourmaline as a petrogenetic indicator mineral: An example from the staurolite-grade metapelites of northwest Maine: American Mineralogist, v. 70, p. 1-15.

Howard, P.F., 1969, The geology of the Elizabeth mine, Vermont: Vermont Geological Survey Economic Geology 5, 73 p.

Irvine, T.N., and Baragar, W.R.A., 1971, A guide to the chemical classification of the common volcanic rocks: Canadian Journal of Earth Sciences, v. 8, p. 523-548.

Kinkel, A.R., Jr., 1967, The Ore Knob copper deposit, North Carolina, and other massive sulfide deposits of the Appalachians: U.S. Geological Survey Professional Paper 558, 58 p.

LaPierre, P.T., 1977, The geology, zoning, and textural features of the Second Pond ore deposit, Blue Hill, Maine: Unpublished M.S. thesis, University of Maine, 75 p.

McKinstry, H.E., and Mikkola, A.K., 1954, The Elizabeth copper mine, Vermont: Economic Geology, v. 49, p. 1-30.

Meyn, H.D., and Palonen, P.A., 1980, Stratigraphy of an Archean submarine fan: Precambrian Research, v. 12, p. 257-285.

Mittwede, S.K., 1984, Tourmalinite, anomalous tourmaline concentration and iron-formation as exploration guides in northwestern Cherokee County, South Carolina: South Carolina Geology, v. 27, no. 1 and 2, p. 6-12.

Morey, G.B., 1978, Lower and Middle Precambrian stratigraphic nomenclature for east-central Minnesota: Minnesota Geological Survey Report of Investigations 21, 52 p.

Nesbitt, B.E., Longstaff, F.J., Shaw, D.R., and Muehlenbacks, K., 1984, Oxygen isotope geochemistry of the Sullivan massive sulfide deposit, Kimberly, British Columbia: Economic Geology, v. 79, p. 933-946.

Pettijohn, F.J., Potter, P.E., and Siever, R., 1972, Sand and sandstone: Springer-Verlag, 618 p.

Plimer, I.R., 1986, Tourmalinites from the Golden Dyke Dome, Northern Australia: Mineralium Deposita, v. 21, p. 263-270.

___, 1987, The association of tourmalinite with stratiform scheelite deposits: Mineralium Deposita, v. 22, p. 282-291.

Plimer, I.R., and Lees, T.C., 1988, Tourmaline-rich rocks associated with the submarine hydrothermal Roseberry Zn-Pb-Cu-Ag-Au deposit and granites in western Tasmania, Australia: Mineralogy and Petrology, v. 38, p. 81-103.

Roberts, W.M.B., 1973, Dolomitization and genesis of Woodcutter's lead-zinc prospect, Northern Territory, Australia: Mineralium Deposita, v. 8, p.35-36.

Schmidt, R.G., 1963, Geology and ore deposits of the Cuyuna North range, Minnesota: U.S. Geological Survey Professional Paper 407, 96 p.

Sims, P.K., Card, K.D., Morey, G.B., and Peterman, Z.E., 1980, The Great Lakes tectonic zone—a major crustal structure in central North America: Geological Society of America Bulletin, v. 91, pt. 1, p. 690-698.

Slack, J.F., Herriman, N., Barnes, R.G., and Plimer, I.R., 1984, Stratiform tourmalinites in metamorphic terranes and their geologic significance: Geology, v. 12, p. 713-716.

Southwick, D.L., Morey, G.B., and McSwiggen, P.L., 1988, Geologic map (scale 1:250,000) of the Penokean orogen, central and eastern Minnesota, and accompanying text: Minnesota Geological Survey Report of Investigations 37, 25 p.

Taylor, B.E., and Slack, J.F., 1984, Tourmalines from Appalachian-Caledonian massive sulfide deposits: Textural, chemical, and isotopic relationships: Economic Geology, v. 79, p. 1703-1726.

Turner, F.T., 1968, Metamorpic petrology, mineralogical and field aspects: McGraw-Hill, 403 p.

Vokes, F.M., 1966, On the possible modes of origin of the Caledonian sulfide ore deposits at Bleikvassli, Nordland, Norway: Economic Geology, v. 61, p. 1130-1139.

White, W.S., and Eric, J.H., 1944, Preliminary report on the geology of the Orange County copper district, Vermont: U.S. Geological Survey Open-File Report, 36 p.